

Cardiac computed tomographic imaging to evaluate myocardial scarring/fibrosis in patients with hypertrophic cardiomyopathy: a comparison with cardiac magnetic resonance imaging

Jennifer I. Berliner · Aya Kino · James C. Carr ·
Robert O. Bonow · Lubna Choudhury

Received: 8 December 2011 / Accepted: 28 March 2012 / Published online: 25 April 2012
© Springer Science+Business Media, B.V. 2012

Abstract Contrast enhanced magnetic resonance imaging (CeMRI) reliably identifies myocardial fibrosis in patients with hypertrophic cardiomyopathy (HCM). However, many patients have contraindications to ceMRI. Previous studies have shown that contrast enhanced multi-detector computed tomography (ceMDCT) can visualize focal scars following myocardial infarction in experimental animals and patients. The purpose of this manuscript is to assess the ability of ceMDCT to detect focal myocardial scars in patients with HCM. Twelve HCM patients underwent ceMRI and ceMDCT. Fibrotic areas of myocardium were defined as focal or diffuse areas of fibrosis. The mean signal intensity in ceMRI and attenuation values in ceMDCT of the fibrotic regions, normal myocardium and left ventricle blood pool contrast were measured using qualitative and quantitative analysis. Focal scar mass was

calculated using both techniques. Focal scars were detected in 9 patients and diffuse fibrosis was visualized in all patients by ceMRI. Differences between normalized SI of normal myocardium and focal scars, normal and diffuse areas of fibrosis, and diffuse fibrosis and focal scars were significant for both ceMRI and ceMDCT ($p < 0.05$). Diffuse fibrosis was poorly visualized by ceMDCT but was detectable using quantitative measurements. CeMDCT has potential to detect focal myocardial scars in patients with HCM who have contraindications to ceMRI study. However, ceMDCT does not enable adequate visualization of diffuse myocardial fibrosis, and thus is less well suited than ceMRI for assessment of total burden of fibrosis. This limitation may be overcome using quantitative methodology.

Keywords Hypertrophic cardiomyopathy · Late gadolinium enhancement · MRI · Late contrast enhanced multidetector CT

Jennifer I. Berliner and Aya Kino contributed equally to this article.

J. I. Berliner
Department of Medicine Veterans Affairs Pittsburgh Healthcare System, Division of Cardiology, University of Pittsburgh Medical Center, Pittsburgh, PA, USA

A. Kino · J. C. Carr
Department of Radiology, Feinberg School of Medicine, Northwestern University, Chicago, IL, USA

R. O. Bonow
Department of Medicine and Feinberg School of Medicine, Center for Cardiovascular Innovation, Northwestern University, 645 N Michigan Ave suite 1006, Chicago, IL 60611, USA

L. Choudhury (✉)
Department of Medicine and Feinberg School of Medicine, Division of Cardiology, Northwestern University, 676 North St Clair Street, Suite 600, Chicago, IL 60611, USA
e-mail: LChoudhury@nmff.org

Introduction

Hypertrophic cardiomyopathy (HCM) is a genetic condition characterized by left ventricular (LV) hypertrophy and hyperdynamic LV systolic function [1, 2]. Patients with HCM have a diverse clinical course, and a subset is at risk of sudden death due to ventricular arrhythmias [3]. Patients with HCM commonly have scarring/fibrosis visualized by contrast enhanced magnetic resonance imaging (ceMRI) despite angiographically normal coronary arteries [4]. Myocardial fibrosis is believed to be a substrate for ventricular arrhythmias in HCM [5]. Pathologic studies have revealed the presence of interstitial as well as replacement fibrosis in the myocardium of patients with HCM [6, 7]. In

a small percentage of patients, extensive scarring may also result in the development of endstage HCM with LV dilatation and systolic heart failure [7]. At the present time, ceMRI is the best noninvasive imaging method to visualize myocardial scarring/fibrosis [4, 8, 9]. However, the presence of pacemakers and/or implantable cardioverter-defibrillators (ICDs), which are often required for management of these patients, currently constitutes a contraindication for MRI. Iodinated radiographic contrast agents are retained in areas of myocardial fibrosis in a similar fashion to that seen with gadolinium contrast enhancement and ceMRI. Contrast enhanced multidetector computed tomography (ceMDCT) has been shown in both animal models and human subjects to correlate well with histology and in demonstrating the extent of myocardial scar after myocardial infarction [10, 11].

We conducted this study to evaluate whether ceMDCT can be used as an alternative imaging modality to identify myocardial scarring/fibrosis in patients with HCM with similar accuracy to ceMRI.

Methods

Patients

The research protocol was approved by the institutional review board at Northwestern University (Chicago, IL, USA) and written informed consent forms were obtained from all subjects. The inclusion criteria included patients with known diagnosis of HCM, defined by left ventricular wall thickness of 15 mm or more detected by echocardiography, in the absence of another condition likely to produce that degree of hypertrophy, who underwent. CeMRI examination showing delayed myocardial who agreed to undergo delayed ceMDCT. The study included 12 patients, with a mean age of 43 (± 13.1) years old. 83 % of the patients were male. Two patients had hypertension and one had both diabetes and hypertension. All patients had stress echocardiography ruling out ischemia, except one patient who had coronary angiography showing LAD stenosis requiring a stent, without infarction. Ejection fraction (EF) % was obtained from MRI and echocardiography reports (Table 1). EF was calculated by Simpson's method and automatically calculate at using a special evaluation software (ARGUS, Erlangen, Germany).

Contrast enhanced MRI

Patients were studied using a 1.5 T MRI scanner (Magnetom Avanto, Siemens Medical Solutions, Erlangen, Germany). All of the ceMRI images were acquired using a multi-slice multi breath-hold 2D phase sensitive inversion recovery

Table 1 Patient demographics

ID	Age	Gender	Hypertrophy type	MRI EF (%)	Echo EF (%)
1	51	M	ASH	67	65
2	24	M	ASH	73	65
3	19	M	ASH	69	75
4	46	M	ASH	57	55
5	37	M	CH	64	65
6	51	F	CH	77	73
7	58	M	ASH*	50	65
8	45	M	CH*	66	55
9	46	M	AH	58	70
10	31	F	ASH	56	65
11	45	M	ASH	59	65
12	63	M	AH	63	65

ASH asymmetric septal hypertrophy, CH concentric hypertrophy, AH apical hypertrophy, EF ejection fraction, * ICD implantable cardioverter defibrillator, MRI magnetic resonance imaging

(PSIR) TurboFLASH protocol covering the left ventricle from base to apex (slice thickness = 6 mm with interslice gap of 4 mm), 10 min after contrast injection with Gadolinium-DTPA (0.2 mmol/kg) using the following imaging parameters: TR = 8 ms, TE:3.2 ms, TI: 248.33 ms (± 74.08), flip angle: 25°, FOV: 380 × 309 mm², matrix: 156 × 256, pixel size 2.0 × 1.5 mm²; slice thickness of 6 mm, bandwidth of 140 Hz per pixel, GRAPPA acceleration factor of 2, k-lines per segment = 25.

Dual source cardiac ceMDCT

Dual-source delayed enhanced multidetector CT (Somatom Definition, Siemens Medical Solutions, Erlangen, Germany), was performed using the following parameters: 120 kVp, 300 mAs, rotation time of 0.330 s, collimation of 2 × 32 × 6 mm, slice thickness of 6 mm, pitch increment of 4 mm and matrix size of 512 × 512. A total of 120 ml of iohexol 350 (Omnipaque™ 350, GE Healthcare, Princeton, NJ, USA) [12] at 5 cc/s was given 15 min before the scan through an antecubital vein, at a rate of 5.0 ml/s. Prospective ECG gating was used such that the CT acquisition occurred during mid diastole at approximately 70 % of the R–R interval. The delayed images were reconstructed in slice thickness, 0.75–1.5 mm; increment of 0.5 mm by using reconstructed using a dedicated medium-soft convolution kernel (B26f). Later these delayed ceMDCT images were reconstructed using a multiplanar reformatting (MPR) post processing algorithm at workstation (Leonardo, Siemens Medical Solutions, Erlangen, Germany) in short axis, with a slice thickness of 6 mm and 4 mm of increment and same spatial orientation to match to the corresponding short axis delayed ceMRI images.

Radiation dose was calculated based on the formula $E = K \times \text{DLP}$ (where $K = 0.014$) [13].

Image analysis

Qualitative analysis

Qualitative interpretation of the ceMRI and ceMDCT images was performed independently by two experienced readers (a cardiologist with 10 years experience in MR imaging and a radiologist with 4 years experience in cardiac MRI and CT) blinded to the information of the other scan. Differences in interpretation were adjudicated by consensus. The images were analyzed using an optimal window setting with typical width/level of 700/100. Scars were classified into two categories based on the visual enhancement pattern on ceMRI: focal and diffuse. Focal scars were characterized as well defined areas of high bright signal intensity (SI) areas with well defined borders, surrounded by healthy myocardium. Diffuse scars were characterized by grayish, intermediate-low signal intensity areas, presenting an ill defined border [14]. Scars were visually classified as focal (“F”) or diffuse (“D”) with (“N”) representing normal myocardium. Therefore, each of the 16 segments in a patient received designations of F, D, and N for focal scar, diffuse scar and normal myocardium respectively, depending on the type of scars in that segment; i.e. one segment can have both F & D if it has both diffuse and focal scar. When all the patients are analyzed, the total number of “F”’s and “D”’s were calculated and compared between ceMDCT and ceMRI.

Reformatted ceMDCT images were analyzed using mediastinal window setting.

Quantitative analysis

Regions of interest were drawn delineating the focal scar area in the short-axis slices for the ceMRI and the ceMDCT images. Focal myocardial scar mass was calculated for both ceMRI and the reconstructed CT images. Focal scar areas of the ceMRI and the ceMDCT images were multiplied by the slice thickness of 6 mm plus 4 mm gap in all slices. Total focal scar mass was calculated assuming a myocardial density of 1.05 g/ml [15]. The mean SI of the scar (delayed enhancement), the remote myocardium and LV cavity were measured in the ceMRI images for quantitative analysis. The SI between focal scars (6 SD thresholds) [16], diffuse scar, (MR gray-scale thresholding with 2 or more SDs above the mean signal intensity for the visually normal remote myocardium) [17], using a commercially available software QMASS (Medis Medical Imaging Systems, Leiden, The Netherlands) and remote healthy myocardium, were normalized to respective values

of the LV cavity for MR images [18]. Similarly, on reconstructed CT images the mean attenuation values in Hounsfield units (HU) of the visualized delayed enhanced areas (focal scars by CT) and remote myocardium and LV cavity were obtained. The ceMDCT images were reviewed blinded to the MR images in terms of visual detection of scar. When a diffuse scar was detected on ceMRI, even though the corresponding areas on CT images did not have visually detectable fibrosis; the area was analyzed by positioning a ROI in order to calculate HU for quantitative analysis. The normalized SI and attenuation values for the areas of myocardial scar (focal and diffuse) were then compared for the two imaging modalities.

The maximal LV wall thickness was also measured in both imaging modalities and compared.

Statistical analysis

Student *t* test, ANOVA, Bland–Altman and linear regression were used to analyze agreement between scar classification and mass detected by ceMRI and ceMDCT. SPSSv17 (Chicago, IL, USA). A *p* value of 0.05 or less was considered to indicate statistical significance.

Results

A total of 12 patients consented to participate in the study. The ceMDCT was performed a mean of 5 months (SD = 3.8 months, range 1–11 months) after ceMRI. Seven patients had asymmetric septal hypertrophy, 3 had concentric LV hypertrophy and 2 had apical hypertrophy. Image quality was compromised in two of the 12 patients who had an ICD implanted between the ceMRI and ceMDCT scans. This caused some streaking artifacts in some areas of myocardium during the delayed ceMDCT, but these patients had scars on ceMRI in regions that were not affected by ICD artifacts on CT. The mean radiation dose was 4.5 mSv (± 0.34).

Sample images for ceMRI and reconstructed ceMDCT images are shown in Figs. 1 and 2.

Results of qualitative analysis of focal scars: Focal scars were detected visually in 9 patients by both ceMDCT and ceMRI. There was no difference in detecting focal scars qualitatively by ceMRI and ceMDCT as the same number of scars were detected and classified as focal scars by both methods (Fig. 3). Focal scars were located predominantly in the septal and inferior segments.

Results of quantitative analysis of focal scars: The total focal scar mass for the ceMRI images and reconstructed short axis ceMDCT images was not significantly different ($p = 0.49$, Fig. 4). There was a significant correlation between the total myocardial mass ($R^2 = 0.91$), as well as

focal scar mass (Fig. 5) detected by both methods ($R^2 = 0.78$). This is also shown at Bland–Altman plot agreement in total myocardial mass and focal scar mass detected by ceMRI and ceMDCT (Fig. 6).

Significant differences in SI between focal and diffuse scars (compared to each other and to the normal myocardium) were identified in the ceMRI images. These differences were also visually apparent, allowing the observers to easily distinguish focal and diffuse myocardial scars from each other and from normal myocardium on ceMRI images (Table 2). Qualitative analysis of diffuse scars: diffuse scars were observed in all patients with ceMRI. There was a significant difference between the mean score for diffuse scars detected qualitatively for ceMRI and ceMDCT (1.42 ± 0.81 vs. 1.25 ± 0.66 , respectively, $p < 0.001$). Ten lesions representing diffuse scars detected by ceMRI were not detected visually on the ceMDCT images. However, the quantitative analysis of the delayed ceMDCT tomograms did detect a significant difference between normal myocardium and both focal and diffuse scars ($p = 0.04$) (Table 2).

There was no significant difference in mean maximum wall thickness measurements between ceMRI and

ceMDCT ($p = 0.83$). The mean maximum wall thickness detected by ceMRI was 25.2 ± 4.95 and 25.5 ± 6.40 mm by ceMDCT.

Discussion

Previous work has demonstrated the utility of delayed ceMRI to evaluate myocardial scarring in patients with HCM [4, 19]. Recently, a case report demonstrated the ability of ceMDCT to detect the presence of the myocardial scarring in patients with HCM [20]. The current study is the first to compare ceMRI to ceMDCT, both qualitatively and quantitatively, for the evaluation of myocardial scarring in patients with HCM. Our data demonstrate that ceMDCT can accurately identify the presence of myocardial scar in patients with HCM and may therefore be an important diagnostic tool, especially in patients who cannot undergo cardiac MRI due to contraindications such as claustrophobia or implanted cardiac devices. A significant finding of this study is the identification of 2 distinct patterns of scarring by ceMRI—focal and diffuse—in patients with HCM. Historically, analysis of myocardial scarring

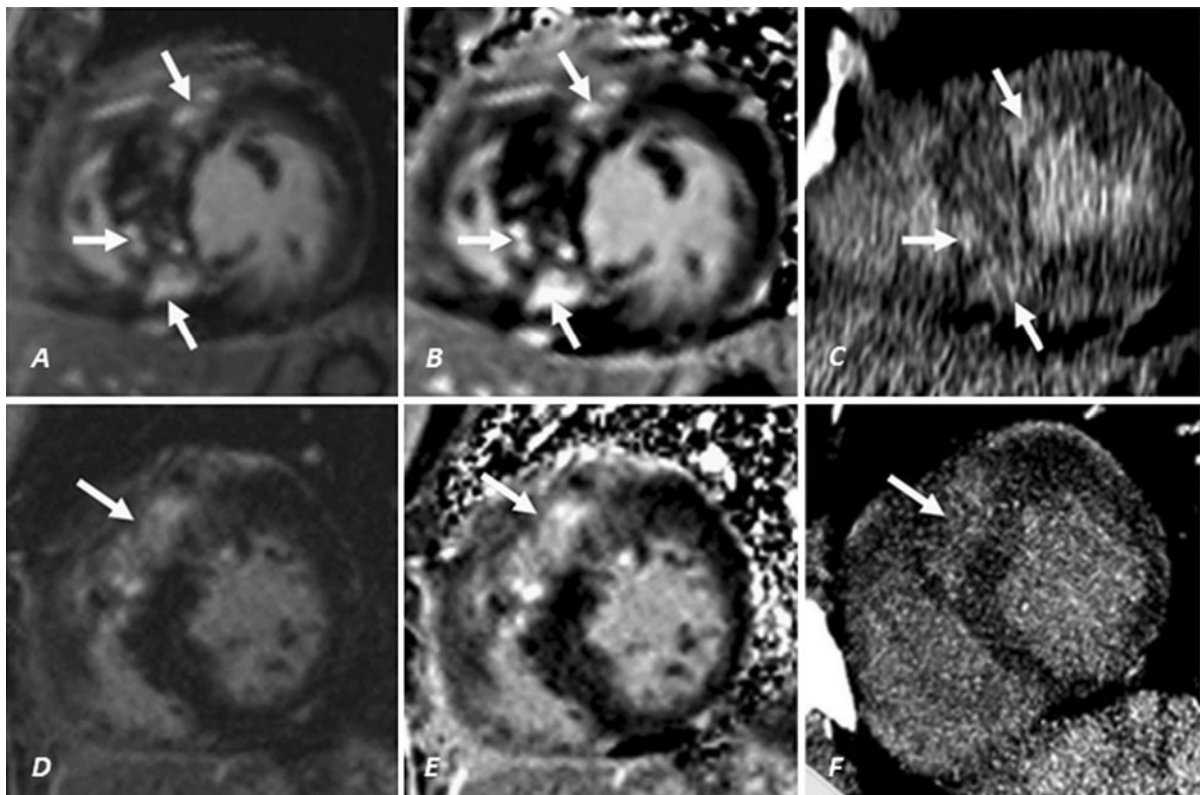


Fig. 1 Asymmetric septal hypertrophy with focal scar—ceMRI (**a** magnitude image; **b** phase sensitive image) and ceMDCT (**c**) reconstructed images of 37 year-old man with asymmetric septal hypertrophy demonstrating multiple focal scars as delayed enhancement within the myocardium (*arrows*) detected in both ceMRI and

ceMDCT. Focal scar of the interventricular septum—ceMRI (**d** magnitude image; **e** phase sensitive image) and ceMDCT (**f**) reconstructed images of 31-year-old woman with focal scarring particularly in the interventricular septum (*arrows*)

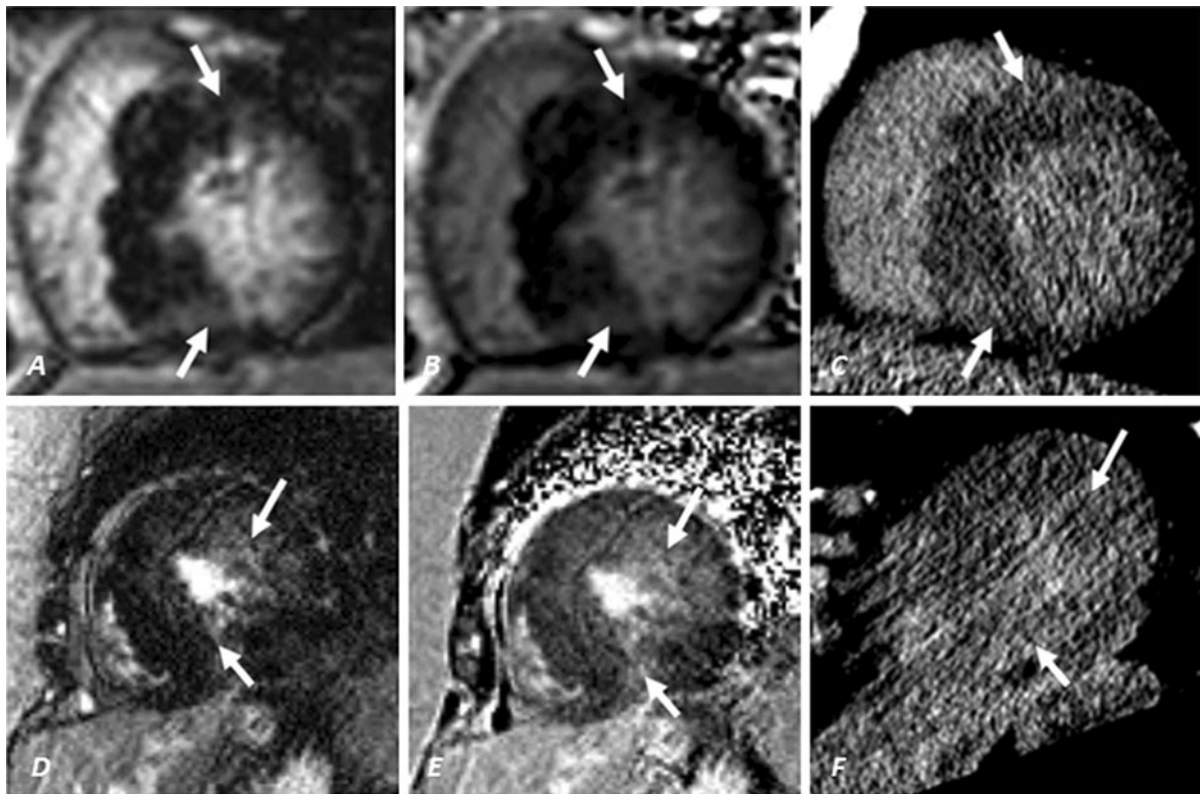


Fig. 2 Asymmetric septal hypertrophy with diffuse scar—ceMRI (a magnitude image; b phase sensitive image) and ceMDCT (c) reconstructed images of 19 year old man with asymmetric septal hypertrophy with diffuse scarring within the myocardium as shown by both ceMRI (white arrows) and not easily appreciated at ceMDCT (gray arrows). Diffuse mid myocardial scar—ceMRI (d magnitude

image; e phase sensitive image) and ceMDCT (f) reconstructed images of a 51-year-old female presenting with concentric left ventricular hypertrophy and diffuse areas of scarring predominantly mid myocardial, from base to apex seen during the ceMRI (white arrows) and not clearly visualized on ceMDCT images (gray arrows)

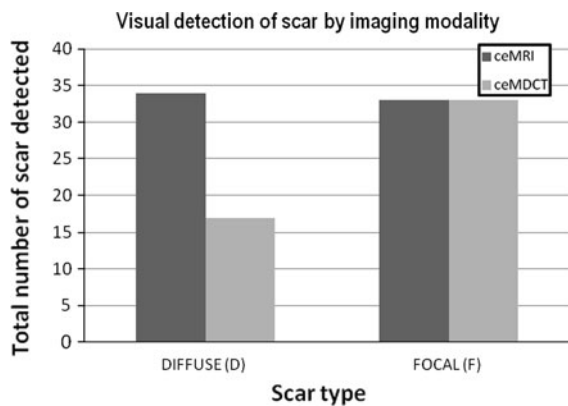


Fig. 3 Total number of scars detected by ceMRI and ceMDCT—the same number of focal scars was detected by both modalities, while ceMDCT detected less diffuse scars

has predominantly focused on identifying and analyzing the presence of focal scarring. However, experience in patients with CAD indicates that ceMRI can identify not only the focal bright areas of myocardial delayed contrast enhancement but also less intense, diffuse gray areas of contrast enhancement [21, 22]. In pathologic studies, it is

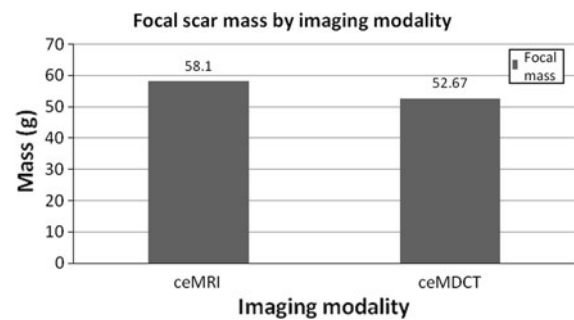


Fig. 4 Mean LV mass and focal scar mass detected by ceMRI and ceMDCT—there was no significant difference between focal scars mass detected by both imaging modalities

well established that patients with HCM have increased interstitial fibrosis, which is a diffuse fibrosis pattern as well as replacement fibrosis or a more focal fibrosis pattern [6, 7]. It is possible that the focal scars visualized by ceMRI represent the replacement fibrosis and diffuse scars relate to interstitial fibrosis. Our data indicate that ceMDCT has an ability to identify the presence of focal scars similar to that of ceMRI, but is limited in the visual detection of diffuse

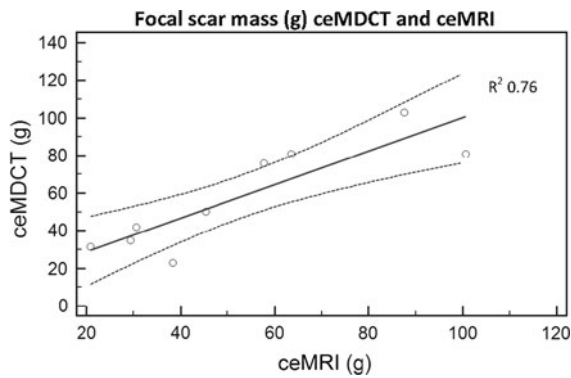


Fig. 5 Correlation between focal scar mass detected by ceMRI and ceMDCT. There was a linear correlation $R^2 = 0.76$ between scar mass detected by both modalities

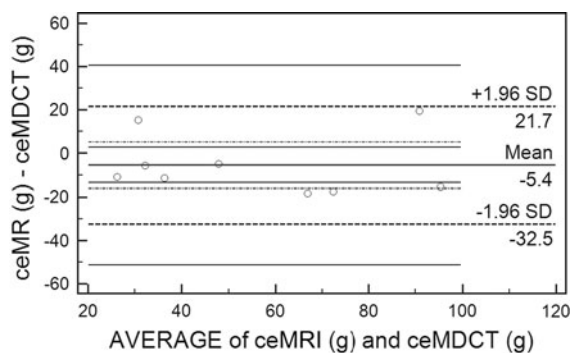


Fig. 6 Bland–Altman plot demonstrating agreement between focal scars mass detected by ceMRI and ceMDCT

myocardial fibrosis. However, our data also demonstrate that the diffuse scarring process can be detected on ceMDCT using additional quantitative measurements.

Imaging of scar/fibrosis in HCM may be useful for risk stratification of patients with HCM [23–25]. Previous studies have reported that ventricular arrhythmias and overall adverse clinical events are more common in HCM patients who have myocardial scar/fibrosis detected by ceMRI than in those who do not [5] and fibrosis detected by CMR has been shown to be an independent predictor of adverse outcomes, all cause mortality and cardiac mortality

[24]. As ceMRI is not feasible in a number of patients with HCM because of the frequent use of implanted metallic cardiac devices in the highest risk patients (or claustrophobia in others), it is important to develop alternative imaging strategies to visualize myocardial scar in these patients. The results of this study indicate that ceMDCT may be useful in identifying the presence and extent of myocardial scarring and fibrosis in patients who are unable to undergo ceMRI. Further research is needed to determine whether the distinction of diffuse versus focal fibrosis visualized by ceMRI in HCM is an important component of risk stratification for patients with this condition.

This study presents several limitations. First, the number of subjects included in the study is small, and further studies with larger number of subjects undergoing ceMRI and ceMDCT to assess both focal and diffuse scarring would be helpful. The small study cohort in this report may be partially offset by the detailed image analysis presented here using high resolution imaging techniques and new quantitative analyses that provide accuracy in the detection of myocardial scar/fibrosis by ceMDCT. The radiation exposure necessary to perform a ceMDCT is a limitation of this imaging modality. Despite this drawback, radiation doses necessary for cardiac CT imaging are continuously being reduced with ongoing technological advances. Although the diffuse fibrosis was visualized using the available ceMRI techniques available at the time of this study, more sophisticated technological advances, including the ability to detect diffuse myocardial fibrosis that is not visible, with ceMRI by T1 mapping are always being developed and may be more effective in quantifying diffuse fibrosis [26]. Finally, we do not have a gold standard in the form of pathologic or biopsy specimens to confirm the ceMRI and ceMDCT data regarding the presence and nature of myocardial scarring, though case reports exist describing such a correlation. A radiologic-pathologic correlation of the different types of scars detected by the noninvasive imaging modalities would be useful in a larger prospective study. A plausible study may include patients undergoing septal myectomy who have septal scarring detected in vivo by preoperative ceMRI and ceMDCT.

Table 2 Signal intensity for ceMRI and Hounsfield units for ceMDCT for normal myocardium, diffuse fibrosis and focal scars

Imaging modality	Normal myocardium	Diffuse fibrosis	Focal scar
ceMRI (normalized SI)	0.326 ± 0.35	0.541 ± 0.31 <i>p</i> = 0.0126 versus normal	0.965 ± 0.25 <i>p</i> = 0.0004 versus normal <i>p</i> = 0.0002 versus diffuse
ceMDCT (normalized HU)	0.658 ± 0.19	0.822 ± 0.21 <i>p</i> = 0.0029 versus normal	1.002 ± 0.16 <i>p</i> = 0.0023 versus normal <i>p</i> = 0.0415 versus diffuse

HU hounsfield units, SI signal intensity

In summary, the results of this study are promising. Delayed ceMDCT studies could be an alternative method for detecting focal myocardial scars in HCM patients who have contraindications for ceMRI study. Although ceMDCT is less well suited than ceMRI for the visual assessment of the total burden of myocardial fibrosis in HCM, quantitative assessment of the presence of diffuse myocardial fibrosis using quantitative methods with ceMDCT may overcome some of its limitations.

Conflict of interest All the authors of the manuscript (Jennifer I. Berliner MD, FACC, Aya Kino MD, James C. Carr, MD, Robert O. Bonow, MD, MACC, Lubna Choudhury, MB BCh, MD, MRCP, FACC) does not have nothing to disclosure and have full control of all primary data and also allow the journal to review the data if requested.

References

- Spirito P, Seidman CE, McKenna WJ et al (1997) The management of hypertrophic cardiomyopathy. *N Engl J Med* 336: 775–785
- Maron BJ, McKenna WJ, Danielson GK et al (2003) American College of Cardiology/European Society of Cardiology clinical expert consensus document on hypertrophic cardiomyopathy. A report of the American college of cardiology foundation task force on clinical expert consensus documents and the European society of cardiology committee for practice guidelines. *J Am Coll Cardiol* 42:1687–1713
- Maron BJ (2002) Cardiology patient pages. Hypertrophic cardiomyopathy. *Circulation* 106:2419–2421
- Choudhury L, Mahrholdt H, Wagner A et al (2002) Myocardial scarring in asymptomatic or mildly symptomatic patients with hypertrophic cardiomyopathy. *J Am Coll Cardiol* 40:2156–2164
- Adabag AS, Maron BJ, Appelbaum E et al (2008) Occurrence and frequency of arrhythmias in hypertrophic cardiomyopathy in relation to delayed enhancement on cardiovascular magnetic resonance. *J Am Coll Cardiol* 51:1369–1374
- Varnava AM, Elliott PM, Mahon N et al (2001) Relation between myocyte disarray and outcome in hypertrophic cardiomyopathy. *Am J Cardiol* 88:275–279
- Maron BJ (1997) Hypertrophic cardiomyopathy. *Lancet* 350: 127–133
- Lima JA, Judd RM, Bazille A et al (1995) Regional heterogeneity of human myocardial infarcts demonstrated by contrast-enhanced MRI. Potential mechanisms. *Circulation* 92:1117–1125
- Moon JC, Sievers B, Pennell DJ et al (2003) Myocardial scarring caused by left ventricular assist device (LVAD) insertion demonstrated by cardiovascular magnetic resonance. *J Cardiovasc Magn Reson* 5:361–363
- Gerber BL, Belge B, Legros GJ et al (2006) Characterization of acute and chronic myocardial infarcts by multidetector computed tomography: comparison with contrast-enhanced magnetic resonance. *Circulation* 113:823–833
- Baks T, Cademartiri F, Moelker AD et al (2006) Multislice computed tomography and magnetic resonance imaging for the assessment of reperfused acute myocardial infarction. *J Am Coll Cardiol* 48:144–152
- Mahnken AH, Katoh M, Bruners P et al (2005) Acute myocardial infarction: assessment of left ventricular function with 16-detector row spiral CT versus MR imaging—study in pigs. *Radiology* 236:112–117
- Christner JA, Kofler JM, McCollough CH (2010) Estimating effective dose for CT using dose-length product compared with using organ doses: consequences of adopting International Commission on Radiological Protection publication 103 or dual-energy scanning. *AJR Am J Roentgenol* 194:881–889
- Moon JC, McKenna WJ, McCrohon JA et al (2003) Toward clinical risk assessment in hypertrophic cardiomyopathy with gadolinium cardiovascular magnetic resonance. *J Am Coll Cardiol* 41:1561–1567
- Sandstede J, Lipke C, Beer M et al (2000) Age- and gender-specific differences in left and right ventricular cardiac function and mass determined by cine magnetic resonance imaging. *Eur Radiol* 10:438–442
- Simor T, Suranyi P, Ruzsics B et al (2010) Percent infarct mapping for delayed contrast enhancement magnetic resonance imaging to quantify myocardial viability by Gd(DTPA). *J Magn Reson Imaging* 32:859–868
- Krombach GA, Niendorf T, Gunther RW et al (2007) Characterization of myocardial viability using MR and CT imaging. *Eur Radiol* 17:1433–1444
- Saito H, Naito H, Takamiya M et al (1991) Late enhancement of the left ventricular wall in hypertrophic cardiomyopathy by ultrafast computed tomography: a comparison with regional myocardial thickening. *Br J Radiol* 64:993–1000
- Maron MS, Appelbaum E, Harrigan CJ et al (2008) Clinical profile and significance of delayed enhancement in hypertrophic cardiomyopathy. *Circ Heart Fail* 1:184–191
- Shiozaki AA, Kim RJ, Parga JR et al (2007) Cardiovascular magnetic resonance in hypertrophic cardiomyopathy. *Arq Bras Cardiol* 88:243–248
- Yan AT, Shayne AJ, Brown KA et al (2006) Characterization of the peri-infarct zone by contrast-enhanced cardiac magnetic resonance imaging is a powerful predictor of post-myocardial infarction mortality. *Circulation* 114:32–39
- Roes SD, Borleffs CJ, van der Geest RJ et al (2009) Infarct tissue heterogeneity assessed with contrast-enhanced MRI predicts spontaneous ventricular arrhythmia in patients with ischemic cardiomyopathy and implantable cardioverter-defibrillator. *Circ Cardiovasc Imaging* 2:183–190
- Kwon DH, Smedira NG, Rodriguez ER et al (2009) Cardiac magnetic resonance detection of myocardial scarring in hypertrophic cardiomyopathy: correlation with histopathology and prevalence of ventricular tachycardia. *J Am Coll Cardiol* 54:242–249
- O'Hanlon R, Grasso A, Roughton M et al (2010) Prognostic significance of myocardial fibrosis in hypertrophic cardiomyopathy. *J Am Coll Cardiol* 56:867–874
- Bruder O, Wagner A, Jensen CJ et al (2010) Myocardial scar visualized by cardiovascular magnetic resonance imaging predicts major adverse events in patients with hypertrophic cardiomyopathy. *J Am Coll Cardiol* 56:875–887
- Iles L, Pflugger H, Phrommintikul A et al (2008) Evaluation of diffuse myocardial fibrosis in heart failure with cardiac magnetic resonance contrast-enhanced T1 mapping. *J Am Coll Cardiol* 52:1574–1580